

## CREATING CALIBRATION CURVES TO DETERMINE SHOCK PRESSURE IN CLINOPYROXENE.

Laura E. JENKINS<sup>\*1,2</sup>, Roberta L. FLEMMING<sup>1,2</sup>, Mark BURCHELL<sup>3</sup>, Kathryn HARRISS<sup>3</sup>, Anne H. PESLIER<sup>4</sup>  
 Roy G. CHRISTOFFERSEN<sup>4</sup>, Jörg FRITZ<sup>5</sup>, and Cornelia MEYER<sup>6</sup>. <sup>1</sup>Department of Earth Sciences, Western University, London, Ontario, Canada <sup>2</sup>Centre for Planetary Science & Space Exploration, Western University, London, Ontario, Canada <sup>3</sup>Centre for Astrophysics & Planetary Science, University of Kent, Canterbury, UK <sup>4</sup>Jacobs, NASA Johnson Space Center (JSC), Houston, Texas, USA <sup>5</sup>Saalbau Weltraum Projekt, Heppenheim, Germany  
<sup>6</sup>Horizontereignis gUG, Charlottenburg, Germany \*Corresponding Author: ljenkin9@uwo.ca

**Introduction:** Impact cratering is an important geological process that occurs on every rocky body in the solar system. It alters the texture and mineralogy of rocks via shock metamorphism.

The peak shock pressures experienced by a rock are traditionally evaluated using qualitative optical methods however, quantitative methods do exist. One such method was developed by Uchizono et al. [1], who used X-ray Diffraction (XRD) to measure lattice strain ( $\epsilon$ ) in several artificially shocked olivine grains using XRD peak broadening as a function of  $\tan\theta$ , where  $\theta$  is the diffraction angle. They plotted the  $\epsilon$  values against the known peak shock pressures experienced by the olivine grains. Using this calibration curve, the precise shock pressure experienced by a grain of olivine can be determined using its measured  $\epsilon$  value [1]. Another method was developed by McCausland et al. [2] and Izawa et al. [3], who used *in situ* XRD to measure strain-related mosaicity (SRM) of olivine in several ordinary chondrites and enstatite in enstatite chondrites, respectively. They plotted these results against the shock stage estimates for these meteorites. Using these plots, meteorites can be assigned to shock stage bins by measuring the SRM of olivine and/or enstatite.

Both methods are useful for evaluating shock metamorphism, however, they have limitations. Uchizono et al.'s [1] calibration curve has been successfully applied to martian meteorites [4], however it can only be applied to olivine-bearing rocks. McCausland et al.'s [2] and Izawa et al.'s [3] SRM method is uncalibrated and is limited to binning meteorites by shock stage. This work aims to expand on both methods by creating calibration curves for clinopyroxene (CPX): one for  $\epsilon$ , similar to Uchizono et al.'s [1] calibration curve for olivine, and one for SRM. This will extend the application of shock calibration methods to a greater variety of rock types. Preliminary results are presented herein.

**Samples:** Three sets of artificially shocked CPX samples were obtained to create the preliminary shock calibration curve.

Augite samples were sent to the University of Kent and were shocked using a two-stage light gas gun (LGG) at the hypervelocity impact facility there [5]. These samples shall herein be referred to as A1, A2, A3, A4, A5, A6, and A7. They were shocked to 8, 22,

31, 49, 66, 91, and 101 GPa, respectively. The corresponding unshocked sample of augite is A0.

Diopside grains from peridotite xenoliths that were artificially shocked by the flat-plate accelerator (FPA) and a vertical gun (VG) at the Experimental Impact Laboratory of NASA-JSC were also used. The samples are herein referred to as EXP2 and HEXP6. HEXP6 was shocked to 40 GPa with an FPA, while EXP2 was shocked up to 20 GPa with a VG.

Samples of gabbro from the Bushveld Igneous Complex that were shocked with an FPA by Meyer et al. (2011) were also obtained [6]. These samples contain diopside. They shall herein be referred to as B1a, B1b, B2, and B3. B1a and B1b were shocked to 30 GPa at 233°K and 293°K, respectively. B2 was shocked to 41 GPa at 293°K, while B3 was shocked to 50 GPa at 293°K.

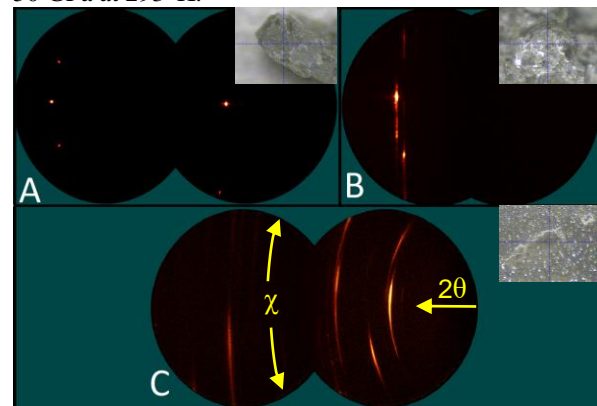


**Fig. 1.** GADDS images from various samples. **A:** GADDS image of spall from A7. This piece of spall is unshocked. **B:** GADDS image from the center of the crater of A2, showing asterism. **C:** GADDS image from HEXP6, showing SRM.  $2\theta$  and  $\chi$  directions are labelled.

**Methods:** Spall from samples A1-A7 were separated based on mass. CPX samples were analyzed *in situ* using a Bruker D8 Discover micro X-ray diffractometer ( $\mu$ XRD) at Western University with a Co K $\alpha$  X-ray source (Co K $\alpha_1$   $\lambda = 1.78897 \text{ \AA}$ ) with a nominal 300  $\mu\text{m}$  beam diameter, Vantec-500 area detector and General Area Detector Diffraction System (GADDS) software, displaying 2D diffraction data similar to that of a Debye-Scherrer film [4][7]. 2D GADDS images were integrated to produce 1D diffraction patterns using

DIFFRAC.EVA. 1D diffraction patterns can be plotted as intensity versus  $\chi$  or intensity versus  $2\theta$  figures, where  $\chi$  is the direction at which the X-ray is diffracted and  $\theta$  is the angle at which the X-ray is diffracted (Fig. 1). For samples shocked with an LGG or VG, the location on the sample where the data were collected is given (Tab. 1).

2D XRD data yields information regarding the texture of analyzed samples. Unshocked, coarse-grained samples yield single diffraction spots in a GADDS image (Fig. 1a), whereas shocked samples will show SRM and asterism (Fig. 1b and Fig. 1c). SRM is the misorientation of subgrains due to non-uniform strain, while asterism occurs when the misoriented subgrains are greater than 10-15  $\mu\text{m}$  in size [8]. In GADDS images SRM is displayed as streaking along Debye rings, while asterism is shown as several spots along Debye rings. SRM was determined by measuring peak width of diffraction peaks in an intensity versus  $\chi$  plot.

$\epsilon$  is determined using Williamson-Hall (WH) plots, which relate peak broadening of a crystal grain's XRD pattern to its grain size and strain [1][9]. A WH plot is created by measuring the width of each diffraction peak as integral breadth ( $\beta$ ) in an intensity versus  $2\theta$  plot, and plotting it against  $\tan \theta$ . From the slope of the WH plot, the  $\epsilon$  of the crystal grain can be calculated (Fig. 2) [1][9]. WH plots with  $R^2$  values less than 0.75 were discarded. The error of each  $\epsilon$  value is the standard error of regression ( $SE_R$ ) of its WH plot.

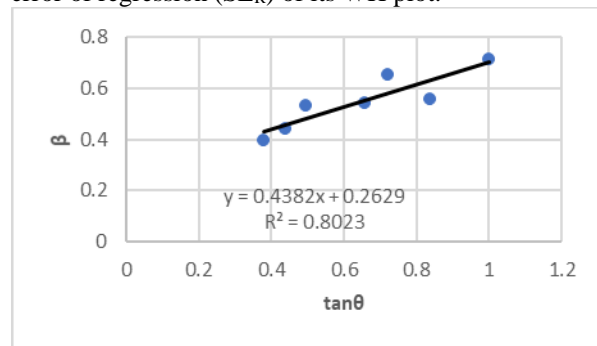


**Fig. 2.** WH plot for sample A1, which was shocked to 8 GPa. Both the formula of the trend line and the  $R^2$  value are given. Using formula [1] Trend line represents  $\beta = 4\epsilon \tan\theta + \beta_0$  (for details see [1]), for which slope ( $4\epsilon$ ) yields  $\epsilon = 0.1096$ .

**Results and Discussion:** A summary of  $\epsilon$  and SRM values and their corresponding shock pressures is given in Tab. 1. Most spall samples displayed  $\epsilon$  and SRM values similar to A0, and thus were deemed to be unshocked. In samples where the impact crater was still visible, targeted areas just outside the crater also showed  $\epsilon$  and SRM values similar to the A0. The  $\epsilon$  and SRM values in targeted areas in the center of craters are higher than A0. For samples shocked by LGG, only the center of the impact crater will accurately reflect

the peak shock pressures it experienced. The rest of the sample, including spall, is heterogeneously shocked.

Asterism was observed in both EXP2 and A2 (Fig. 1b), which were both shocked to up to 20 GPa. Samples that were shocked to higher shock pressures by FPA (HEXP6 and B3) simply showed SRM (Fig. 1c). Whether or not a sample will display asterism or SRM may be due to the level of shock pressure experienced. Another possible explanation is that the shock delivery method may affect whether or not a sample displays asterism, as EXP2 and A2 (showing asterism) were shocked with a VG and LGG, while HEXP6 and B3 (showing SRM) were shocked by FPA. Samples A4-A7 were too fragmented to identify impact craters in order to test this hypothesis.

**Tab. 1.** Values of  $\epsilon$  and SRM for samples and spot locations targeted by  $\mu$ XRD relative to impact crater, if applicable.

Sample	Shock Pressure (GPa)	$\epsilon \pm SER$ (%)	Average SRM (°)	Location relative to crater
A0	0	0.0866±0.0677	0.46	No crater
A1	8	0.1096±0.0973	2.16	Centre
A1	8	0.0613±0.1104	0.55	Edge
EXP2	20	0.0275±0.0027	0.49	Unknown
A2	22	0.0845±0.0153	N/A	Edge
A3	31	0.0892±0.0027	0.59	Spall
HEXP6	40	0.2485±0.0171	7.22	No crater
B3	50	0.3173±0.1198	4.72	No crater
A7	101	0.0711±0.0654	0.56	Spall
A7	101	0.1124±0.0656	N/A	Spall
A7	101	0.0726±0.0601	0.61	Spall
A7	101	0.0771±0.0480	0.61	Spall
A7	101	0.0684±0.0496	0.57	Spall

**Conclusions and Future Work:** From the currently available data, an accurate and precise shock calibration curve cannot yet be presented. More data will be collected to yield a representative calibration curve. Data from the center of the crater of A2 will be collected to determine  $\epsilon$  value. CPX grains will be identified in samples B1a, B1b, and B2, for *in situ* XRD determination of  $\epsilon$  values. Data for B3 and A1 will be re-collected to decrease error. Once completed, this calibration curve will enable quantitative estimates of peak shock pressure for any rock types containing CPX.

**References:** [1] Uchizono et al. (1999) *Mineral. J.*, 21, 15-23. [2] McCausland et al. (2010) *AGU Fall Meeting*, Abs. # P14C-031. [3] Izawa et al. (2011) *MAPS*, 46, 638-651. [4] Jenkins et al. (2019) *MAPS accepted*. [5] Hibbert et al. (2017) *Procedia Engineering*, 204, 208-214. [6] Meyer et al. (2011) *MAPS*, 46, 701-718. [7] Flemming (2007) *CJES*, 44, 1333-1346. [8] Vinet et al. (2011) *Amer. Mineral.*, 96, 486-497. [9] Williamson and Hall (1953) *Acta Metall.*, 1, 22-31.